Clin Orthop Relat Res (2017) 475:998–1008
DOI 10.1007/s11999-016-5038-2

Clinical Orthopaedics and Related Research®
A Publication of The Association of Bone and Joint Surgeons®

SYMPOSIUM: 2016 BERNESE HIP SYMPOSIUM

Increased Hip Stresses Resulting From a Cam Deformity and Decreased Femoral Neck-Shaft Angle During Level Walking

K. C. Geoffrey Ng MASc, Giulia Mantovani PhD, Mario Lamontagne PhD, Michel R. Labrosse PhD, Paul E. Beaulé MD, FRCSC

Published online: 31 August 2016

Abstract

Background It is still unclear why many individuals with a cam morphology of the hip do not experience pain. It was recently reported that a decreased femoral neck-shaft angle may also be associated with hip symptoms. However, the effects that different femoral neck-shaft angles have on hip stresses in symptomatic and asymptomatic individuals with cam morphology remain unclear.

Questions/purposes We examined the effects of the cam morphology and femoral neck-shaft angle on hip stresses during walking by asking: (1) Are there differences in hip stress characteristics among symptomatic patients with cam morphology, asymptomatic individuals with cam morphology, and individuals without cam morphology? (2) What are the effects of high and low femoral neck-shaft angles on hip stresses?

Methods Six participants were selected, from a larger cohort, and their cam morphology and femoral neck-shaft angle parameters were measured from CT data. Two participants were included in one of three groups: (1) symptomatic with cam morphology; (2) asymptomatic with a cam morphology; and (3) asymptomatic control with no cam morphology with one participant having the highest femoral neck-shaft angle and the other participant having the lowest in each subgroup. Subject-specific finite element models were reconstructed and simulated during the stance phase, near pushoff, to examine maximum shear stresses on the acetabular cartilage and labrum.

Results The symptomatic group with cam morphology indicated high peak stresses (6.3–9.5 MPa) compared with the asymptomatic (5.9–7.0 MPa) and control groups (3.8–4.0 MPa). Differences in femoral neck-shaft angle influenced both symptomatic and asymptomatic groups; participants with the lowest femoral neck-shaft angles had higher peak stresses in their respective subgroups. There were no differences among control models.

Conclusions Our study suggests that the hips of individuals with a cam morphology and varus femoral neck angle may be subjected to higher mechanical stresses than those with a normal femoral neck angle.

Clinical Relevance Individuals with a cam morphology and decreased femoral neck-shaft angle are likely to experience severe hip stresses. Although asymptomatic

One or more authors (ML, PEB) have received funding from the Canadian Institutes of Health Research (97778A). One or more authors (ML) have received funding from the Natural Sciences and Engineering Research Council of Canada (106769-2013).
All ICMJE Conflict of Interest Forms for authors and *Clinical Orthopaedics and Related Research*® editors and board members are on file with the publication and can be viewed on request.
Clinical Orthopaedics and Related Research® neither advocates nor endorses the use of any treatment, drug, or device. Readers are encouraged to always seek additional information, including FDA-approval status, of any drug or device prior to clinical use.
Each author certifies that his or her institution has approved the human protocol for this investigation, that all investigations were conducted in conformity with ethical principles of research, and that informed consent for participation in the study was obtained.
This work was performed at the Human Movement Biomechanics Laboratory, University of Ottawa, and at The Ottawa Hospital, Ottawa, Ontario, Canada.

K. C. G. Ng, M. Lamontagne, M. R. Labrosse
Department of Mechanical Engineering, University of Ottawa, Ottawa, ON, Canada

G. Mantovani, M. Lamontagne
School of Human Kinetics, University of Ottawa, Ottawa, ON, Canada

M. Lamontagne, P. E. Beaulé (✉)
Division of Orthopaedic Surgery, University of Ottawa, Ottawa, ON, Canada
e-mail: pbeaule@toh.ca; pbeaule@ottawahospital.on.ca

participants with cam morphology had elevated stresses, a higher femoral neck-shaft angle was associated with lower stresses. Future research should examine larger amplitudes of motion to assess adverse subchondral bone stresses.

Introduction

The pathomechanism of the cam-type hip morphology, which in some patients is associated with femoroacetabular impingement (FAI), has been intensely investigated to better understand anatomic and functional parameters associated with symptomatology. The cam deformity, characterized by an aspherical femoral head-neck junction, has been suggested as a cause of labral-chondral damage as well as an early cause for hip osteoarthritis [11, 17]. Several studies suggest that a severe cam deformity, as defined by larger alpha angles, could indicate which individuals may be at risk of developing early hip pain and arthritis [1, 22]. Although many symptomatic individuals with a cam morphology experienced different hip kinematics, notably during level walking [21] and maximal squatting [23, 24], other individuals with a cam morphology may not experience any clinical signs or symptoms [2, 12, 13, 19, 22, 33, 45]. In addition to elevated alpha angles, it was recently noted that a decreased femoral neck-shaft angle might be indicative of early symptoms as well [13, 33, 34, 45]; however, it is unclear what combined effects a large cam morphology and decreased femoral neck-shaft angle have on resultant hip stresses. To our knowledge, no study has incorporated these subject-specific anatomic parameters with computational, finite element methods to determine the effects on mechanical hip stresses.

According to a recent systematic review on finite element simulations of cam FAI [36], there has been limited work pertaining to finite element simulations that examine cam FAI and, moreover, many of the previous studies used idealized hip geometries [8, 15] as opposed to models reconstructed from subject-specific imaging data. It has also been demonstrated that subchondral bone density is higher in individuals with a symptomatic or asymptomatic cam morphology [52, 53]; however, previous finite element simulations neglected subject-specific bone material properties. Previous finite element studies also attempted to delineate pathomechanics of cam FAI using hip reaction loads from instrumented hip prostheses [8, 15, 18] or from inverse dynamics [37], which is typically limited to external and inertial forces and neglects muscle activity [26, 54]. Because muscles contribute greatly to hip contact forces, it may be more appropriate to implement rigid body dynamics and musculoskeletal modeling (including gravitational, inertial, and muscle forces) to calculate joint contact loads.

Because elevated mechanical stresses in the subchondral bone may play a pathomechanical role in cam FAI [42, 52, 53], subject-specific input parameters (perhaps including geometries, material properties, joint loading) are critical to adequately represent a patient demographic. It would also be necessary to examine hip stresses in individuals with an asymptomatic cam morphology to determine if stress magnitudes and distributions of these individuals are comparable to either an at-risk, symptomatic population or healthy control population without cam morphology.

The purpose of this study therefore was to examine the combined effects of the cam morphology and femoral neck-shaft angle on hip stresses during level walking. We specifically addressed two research questions: (1) Are there any differences in hip stress characteristics among patients with cam morphology, asymptomatic individuals with cam morphology, and control individuals without cam morphology? (2) What are the effects of a high or low femoral neck-shaft angle on hip stresses for each respective subgroup?

Patients and Methods

Six male participants (n = 6, age = 32 ± 7 years, body mass index = 26 ± 3 kg/m^2), from a larger patient cohort in a prior study of cam morphology [33], were recruited through the senior orthopaedic surgeon's clinical practice (PEB). Because cam morphology has been more prevalent in younger, athletic males [11], the six participants recruited for this study were male as well. Each participant underwent pelvic imaging using conventional CT scanners (Acquilion; Toshiba Medical Systems Corporation, Otawara, Japan; or Discovery CT750; GE Healthcare, Mississauga, Ontario, Canada) to confirm if they had cam morphology, as indicated by either an axial 3:00 or radial 1:30 alpha angle greater than 50.5° or 60°, respectively [38, 44] (Fig. 1). Participants were scanned in a supine position with a calibration phantom (Model 3; Mindways Software, Austin, TX, USA) placed under the lumbar vertebra for bone mineral densitometry. Participants from the earlier study cohort who initially presented with clinical symptoms, impingement sign, and a cam morphology on CT images were considered as symptomatic participants and candidates for surgery. The other participants were recruited as volunteers who had no hip pain or clinical impingement signs and were unaware whether they had a cam morphology. From these volunteers, participants who showed a cam morphology on CT images but did not present with clinical signs or symptoms were considered asymptomatic, whereas participants with no cam morphology and no clinical signs or symptoms were considered

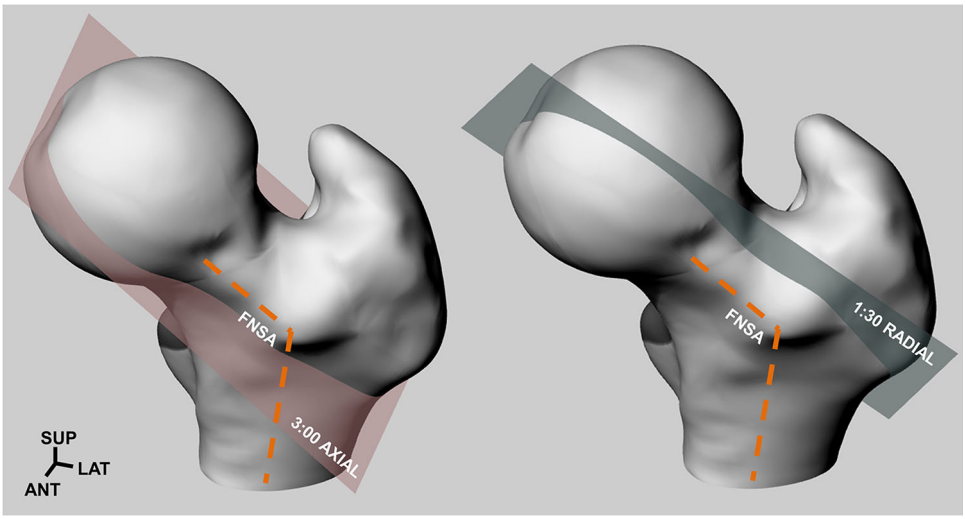

Fig. 1 The cam morphology was determined by an alpha angle greater than 50.5° or 60° either in the 3:00 axial plane (left) or 1:30 radial plane (right), respectively. The femoral neck-shaft angle (FNSA) was also determined to examine the effects of a high and low femoral neck-shaft angle on each participant group. SUP = superior; LAT = lateral; ANT = anterior.

Table 1. Summary of clinical assessments and measured anatomic parameters for each symptomatic, asymptomatic, and control participant with high (H) and low (L) femoral neck-shaft angle

Participant	Age (years)	Body mass index (kg/m^2)	HOOS pain (%)	WOMAC pain (%)	Axial 3:00 alpha angle (°)	Radial 1:30 alpha angle (°)	Femoral neck-shaft angle (°)
Symptomatic H	25	25	53	55	51	63	125
Symptomatic L	33	22	65	80	58	64	119
Asymptomatic H	28	27	100	100	52	66	134
Asymptomatic L	44	27	100	100	56	70	123
Control H	32	26	100	100	44	56	132
Control L	30	29	100	100	41	52	124

HOOS = Hip Disability and Osteoarthritis Outcome Score; H = high femoral neck-shaft angle; L = low femoral neck-shaft angle.

control subjects. Each participant's alpha angles were assessed by a senior-level musculoskeletal radiologist (KSR), where for each symptomatic, asymptomatic, or control participant, the affected side was defined by the hip with symptoms, higher alpha angle, or smaller alpha angle, respectively. Each participant's affected hip underwent subsequent MRI (MAGNETOM Symphony; Siemens Healthcare GmbH, Erlangen, Germany) to determine cartilage thickness and labral contours. Any participant with a history of a major lower limb injury or musculoskeletal abnormality was excluded.

In addition to the cam morphology, the femoral neck-shaft angle of each participant's affected hip was measured from their CT data [33] using a DICOM viewer (Onis 2.4; DigitalCore, Tokyo, Japan) to determine whether the symptomatic group had a decreased femoral neck-shaft angle, an anatomic characteristic associated with FAI symptomatology [33, 34] (Fig. 1). Lateral center-edge angles were measured as well and confirmed to be normal ($\leq 39°$). Participants also completed pain questionnaires—Hip Disability and Osteoarthritis Outcome Score (HOOS) and WOMAC—to assess any subjective differences in symptoms. We expected the symptomatic group to have lower pain questionnaire scores compared with the asymptomatic and control groups (which should have scores near 100%). Based on the resultant anatomic and clinical indications, the larger cohort from the aforementioned earlier study consisted of 12 symptomatic, 17 asymptomatic, and 14 control participants [33]. For this study, we selected two participants for each of the three groups from the larger cohort—one participant with the highest femoral neck-shaft angle and one with the lowest femoral neck-shaft angle for each of the symptomatic, asymptomatic, and control groups (Table 1). The study protocol was approved by the university and hospital research institute ethics boards. Participants provided informed consent before the study and all investigations were conducted ethically in conformity with research principles.

Before motion analysis, in efforts to minimize skin artifacts and pelvic misalignment during motion capture, surface radioopaque markers were placed onto each participant's pelvic landmarks before CT imaging at the left and right anterosuperior iliac spines and posterosuperior

iliac spines. Each participant performed level walking trials, at a self-selected pace, in the motion capture environment. Three-dimensional kinematics were recorded using a 10-camera motion capture system (MX-13; Vicon, Oxford, UK) with retroreflective markers placed on anatomic landmarks according to a modified Plug-in-Gait model [28]. Ground reaction forces of each participant's affected leg, during single stance, were captured using two stationary force plates (FP4060-08; Bertec, Columbus, OH, USA). The trajectories were filtered (Woltring, MSE = 15 mm^2) using motion analysis software (Nexus 1.8; Vicon) and ground reaction forces were filtered (zero-lag, fourth-order Butterworth, cutoff frequency 6 Hz) using numerical computational software (MATLAB R2014a; MathWorks, Nantick, MA, USA).

Muscle and hip contact forces were estimated using a musculoskeletal modeling program (OpenSim 3.1; SimTK, open source program). We adapted a model that consisted of the torso and lower body segments [9], where the hip and lumbar spine were modeled as ball-and-socket joints, which contributed to a total of 29 degrees of freedom and 92 musculotendinous actuators [28]. Muscle forces were computed using a static optimization approach with a quadratic cost function [31] and resultant three-dimensional hip contact forces were calculated and expressed in the pelvic reference system [63].

Each participant's affected hip model was manually segmented from their CT data using image segmentation software (3D-Doctor 4.0; Able Software Corp, Lexington, MA, USA), including slices from the superior iliac crest to the proximal femur (Fig. 2A). The MRI was manually registered and centered on four control points of the target CT images, where the deepest width and depth of the acetabulum and the femoral head center were denoted as registration landmarks. The midpoint between the femoral and acetabular cartilages and their thicknesses were determined. The femoral cartilage, acetabular cartilage, and labrum were manually segmented. None of the participants indicated signs of osteoarthritis or joint space narrowing; therefore, cartilage was modeled as a smooth layer with no surface discrepancies. The segmented models were then resurfaced to reduce geometric artifacts using computer-aided design software (SolidWorks; Dassault Systèmes, Concord, MA, USA). Anatomic hip parameters of the resurfaced models were measured using computer-aided design software and compared with the original CT data to confirm the accuracy of the resurfacing and modeling procedure [35].

Each participant's hip assembly was imported into finite element analysis software (ANSYS 12.1; ANSYS Inc, Canonsburg, PA, USA) and meshed with tetrahedral, SOLID187 elements. Bone material properties were based on subject-specific apparent density using the calibration

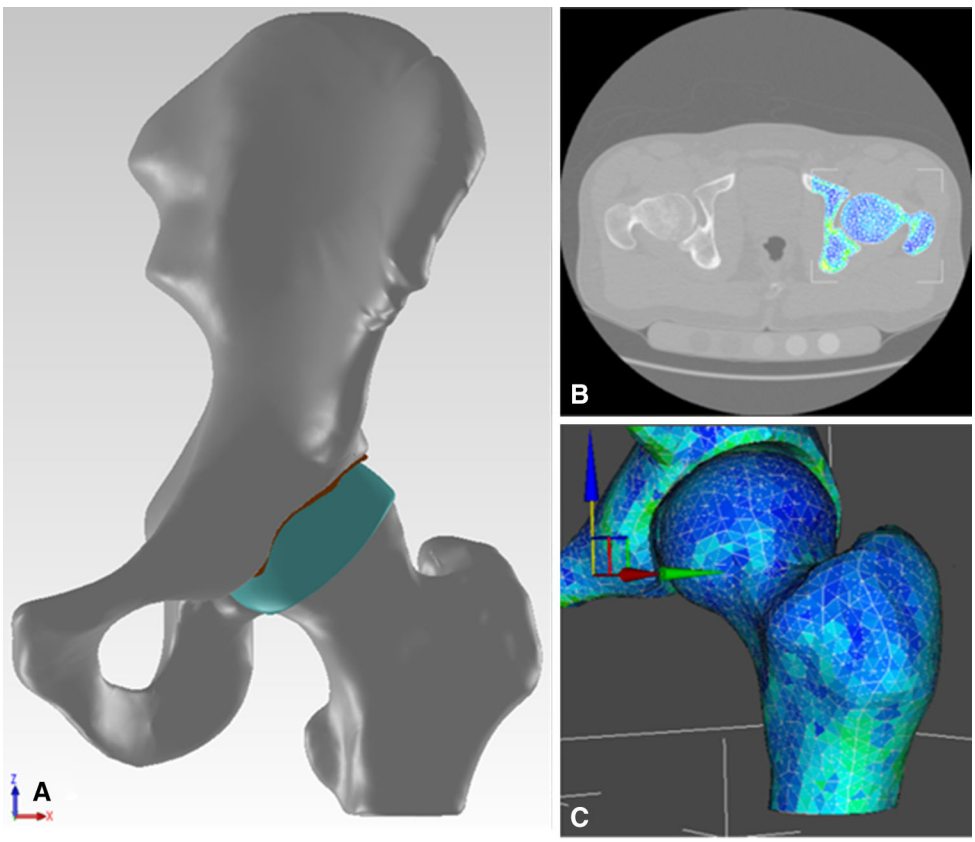

Fig. 2A–C Frontal view of the segmented left hip assembly, from the superior iliac crest to the proximal diaphysis (**A**). The segmented model was resurfaced to reduce geometric artifacts and bone material properties were determined from a density-elasticity relationship that assigned a unique elastic modulus to each individual element (**B**), that resulted in heterogeneous, isotropic bone models (**C**).

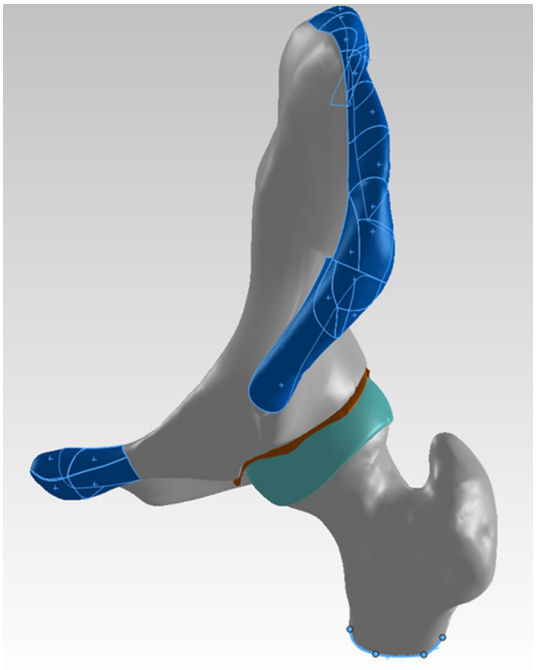

Fig. 3 Boundary conditions were fixed at the pubic symphysis and iliac crest, from the anterosuperior iliac spine to the posterosuperior iliac spine. The femur was oriented according to the kinematics data and was permitted to translate in the loading direction.

phantom and quantitative mapping. Meshes were first imported into the bone density mapping software (Bonemat v3.1; Istituto Ortopedico Rizzoli, Bologna, Italy) and a density-elasticity relationship assigned unique elastic moduli to individual elements (Fig. 2B), for each individual participant model, based on the conversion from the densitometry calibration (ρ_{CT}) to the corrected density (ρ_{ash}), resulting in heterogeneous, isotropic bone models (Fig. 2C) [47, 56]. Cartilage and labrum were modeled as Neo-Hookean, hyperelastic materials [16, 40] with constant hydrostatic pressure (Keyopt[6] = 1, hyperelasticity).

Bone and soft tissue models started with an element size of 3 and 2 mm, respectively, and were further refined to ensure mesh sensitivity. Mesh convergence was considered adequate if the change in stress magnitudes was less than 5% with increasing element refinement. Unaveraged stresses were also compared with averaged integration point results to ensure that the meshes were sufficiently refined. (The smallest resultant element size for the cartilage model was 0.22–0.74 mm.) Contacts between femoral and acetabular cartilages were modeled with a frictional coefficient of 0.01 [57]. Boundary conditions were fixed at the pubis symphysis and iliac crest (from anterior to posterior superior iliac spines) (Fig. 3). The femur model was oriented using the kinematics data during the loading condition and was permitted to translate in the loading direction [16, 37]. A quasistatic loading scenario, using the highest resultant hip forces during terminal stance, was selected for comparison with hip contact forces applied at the femoral head. Because cartilage may be most susceptible to shear stresses under quasistatic loading [27], maximum shear stresses were examined on each participant's acetabular cartilage and labrum to examine adverse loading conditions [15, 37]. A process flowchart from subject-specific input data to resultant hip stresses is summarized (Fig. 4).

Results

The symptomatic and asymptomatic models showed higher maximum shear stresses than the controls. Both symptomatic participants indicated peak maximum shear stresses on the anterolateral cartilage (6.3–9.5 MPa), but also secondary posteroinferior stresses (Fig. 5). Both asymptomatic participants showed moderate stress magnitudes in the superior and posterior cartilage (5.9–7.0 MPa), whereas the controls experienced the lowest stresses with more well-conforming contacts and dissipated distributions along the superior and posterior domes as well (3.8–4.0 MPa; Fig. 5).

Differences in femoral neck-shaft angle influenced both cam morphology groups. The symptomatic participant with the lower femoral neck-shaft angle (119°) had the highest maximum shear stress in the anterolateral cartilage (9.5 MPa; Fig. 6) with a high secondary peak stress in the posterior region (7.9 MPa) as well, whereas the symptomatic participant with the higher femoral neck-shaft angle (125°) showed a lower magnitude (6.3 MPa). The asymptomatic participant with the lowest femoral neck-shaft angle (123°) also had slightly higher peak stress (7.0 MPa) than the asymptomatic participant with the highest femoral neck-shaft angle (134°, 5.9 MPa). There were no substantial differences between the two controls.

Discussion

It is unclear why certain individuals with cam deformities develop progressive degenerative changes and symptoms, whereas others remain asymptomatic for most of their lives [12, 19, 46, 55]. Gaining a better understanding of stresses in asymptomatic hips can provide critical insights into those who are at risk of arthritic changes. In an effort to address differences in the FAI population, we incorporated subject-specific anatomic parameters, geometries, material properties, and joint loading to determine if stresses resulting from an asymptomatic morphology share similarities with symptomatic or healthy individuals. We examined if decreased femoral neck-shaft angles could explain early symptoms resulting from adverse loading

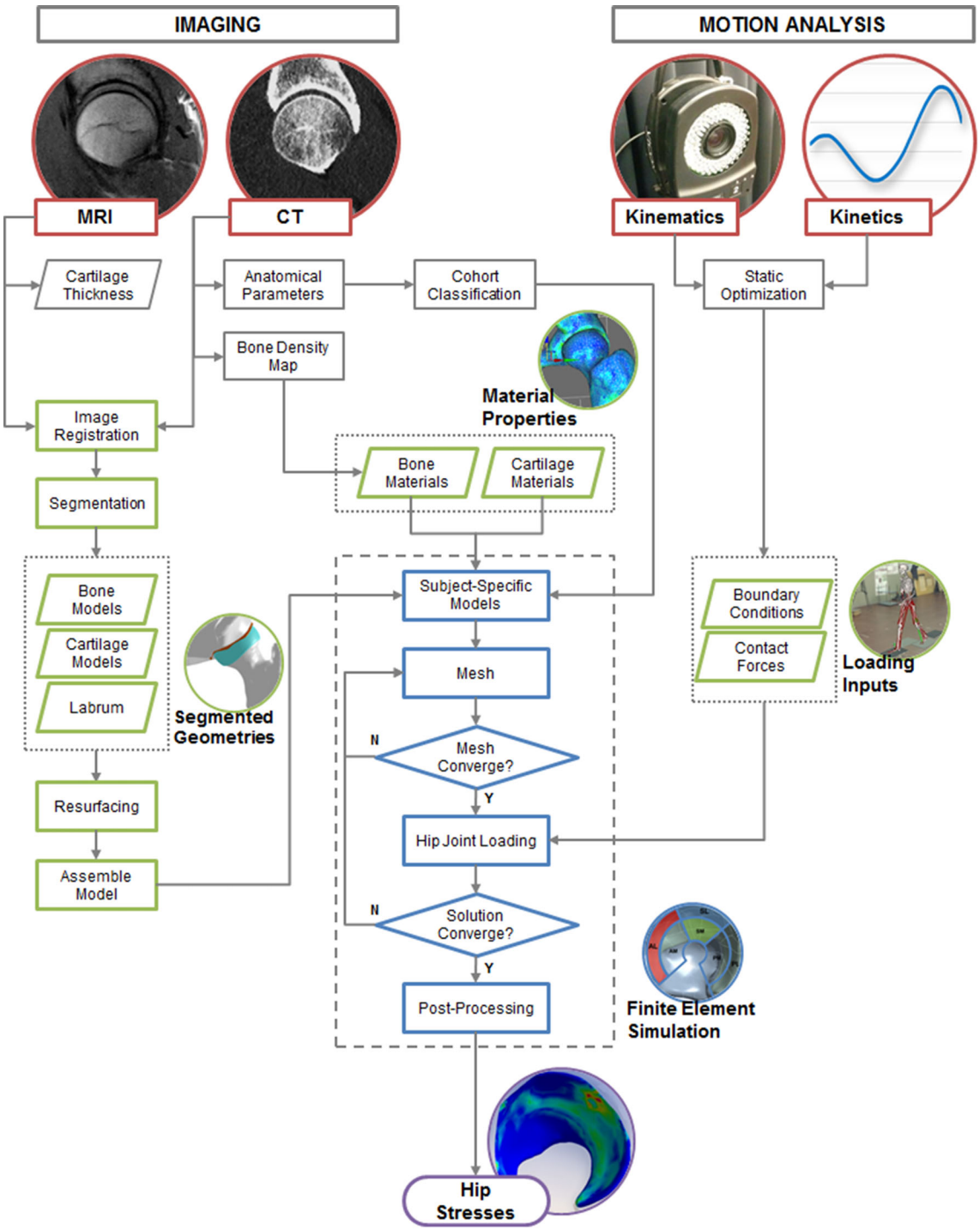

Fig. 4 Process flowchart showing subject-specific input data used for the finite element simulations. The subject-specific hip geometries, material properties, and contact loads were combined and simulated to determine resultant hip stresses.

conditions. Although asymptomatic participants had elevated stresses, a higher femoral neck-shaft angle was associated with lower stresses despite cam morphology.

Our study had certain limitations. First, there was slight overlap in femoral neck-shaft angles between the symptomatic and asymptomatic groups that resulted in overlapping peak hip stresses as well. None of our symptomatic participants had a valgus neck to directly compare with the upper limits of the asymptomatic and control groups (134° and 132°, respectively), whereas similarly,

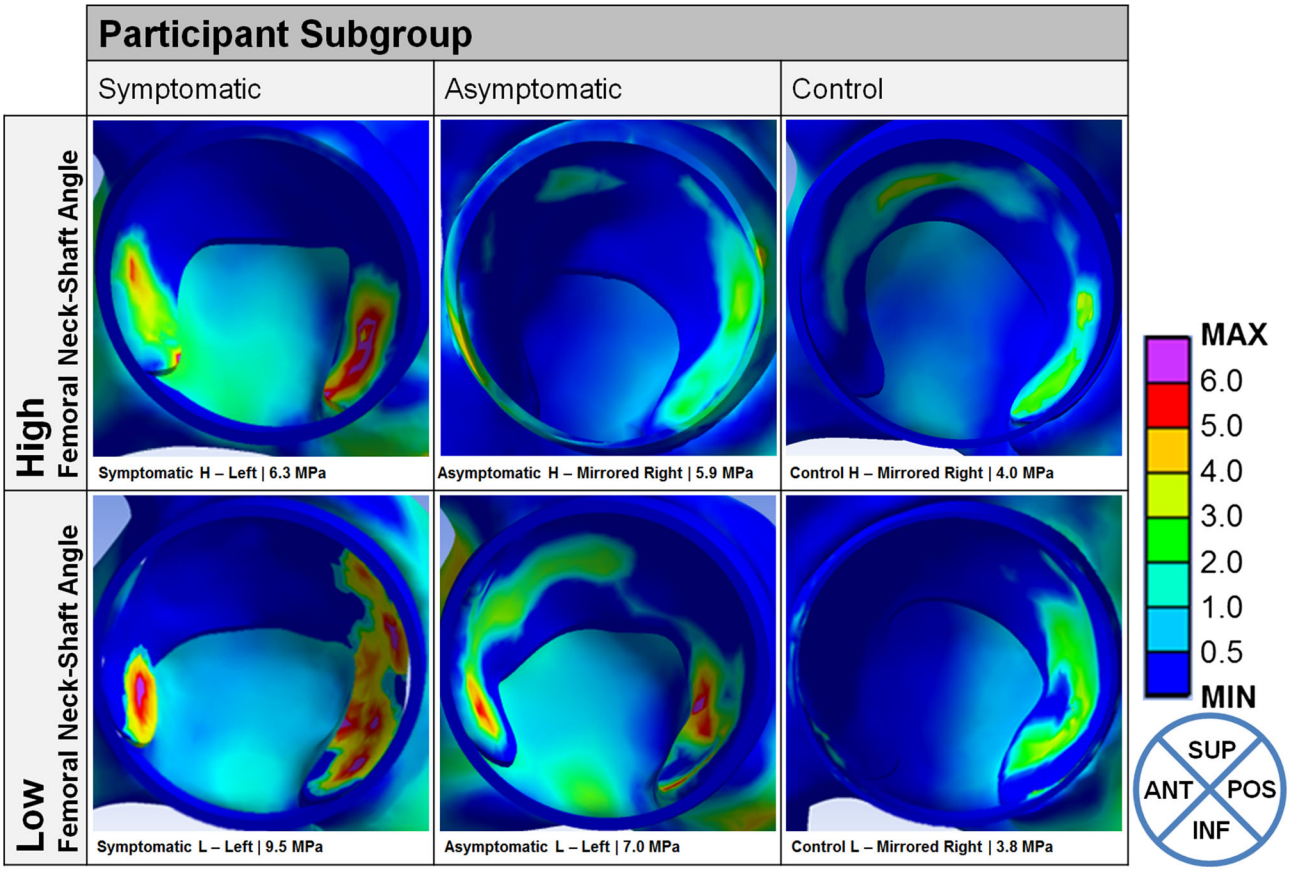

Fig. 5 Sagittal view of the acetabular cartilage and labrum, from the resultant finite element simulations, showing the maximum shear stress distributions for each symptomatic, asymptomatic, and control participant with the highest (H = top row) and lowest (L = bottom row) femoral neck-shaft angle. The reference locations are denoted by anterior (ANT), posterior (POS), superior (SUP), and inferior (INF).

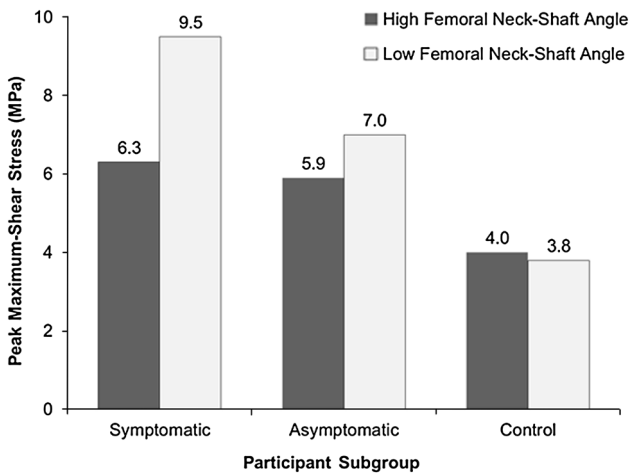

Fig. 6 Graph indicating the peak maximum shear stress for each symptomatic, asymptomatic, and control participant with the highest and lowest femoral neck-shaft angle.

our asymptomatic and control participants did not have varus angles. The participants were selected from a larger cohort (n = 43) that examined differences in anatomic parameters among symptomatic, asymptomatic, and control participants [33]. From that study, the femoral neck-shaft angles of the asymptomatic (127° ± 3°; 123°–134°) and control groups (128° ± 2°; 124°–132°) were higher in comparison with the symptomatic group (123° ± 2°; 119°–125°; $\eta^2 = 0.496$, $p < 0.001$) [33]. It was interesting to note that higher stresses were not necessarily dependent on participant group or symptoms, but perhaps were more associated with femoral neck-shaft angle and a cam morphology. This might also further support the concept that a higher femoral neck-shaft angle decreases the risk of early symptoms [10, 33, 34, 49, 50]. We also accounted for the highest and lowest femoral neck-shaft angles in each group as opposed to examining the largest and smallest cam deformities. Second, certain limitations were imposed by the small sample size. We captured the upper and lower neck angles, but a larger sample size would increase the robustness and differences among the subgroups, which may further delineate intersubject variability and correlate impingement severities with associated anatomic parameters (cam morphology and femoral neck-shaft angle). As a

result of this smaller sample size, we also did not match for body mass index (BMI) between subgroups. We had a small BMI range for each subgroup and thus were unable to observe the effects of varying BMI on hip stresses. Furthermore, because the cam morphology is more prevalent in males [11, 13], our larger cohort that we selected these participants from consisted solely of male participants [33]. Increasing the sample size and including female participants could examine functional and anatomic variances.

Additional limitations of the study include that hip contact forces were determined using static optimization [39, 41]. Previous studies indirectly validated and compared their results with contact forces from instrumented prostheses [7, 14, 26]. Our contact forces were marginally higher than those from instrumented prostheses, but differences in population characteristics, age, walking speed, and activity level should be considered [7, 25, 28, 58, 61]. Fourth, although we improved subject-specific bone material properties to examine FAI, we did not examine biphasic cartilage properties or consolidation, which should be considered in future studies along with dynamic responses [3, 27, 51]. Although subject-specific bone densities were mapped onto individual elements, resulting in heterogeneous bone models, another limitation may be the isotropic property. Isotropy is a conventional material property when implementing subject-specific bone density mapping for heterogeneous components; however, future steps should consider anisotropic or orthotropic properties to simulate the material behavior of bone. Fifth, capsular ligaments and muscle lines of action were not included in the model, because we focused on the contributions of the bony morphology to adverse contact loading. Taut hip ligaments would properly seat the femoral head into the acetabulum at more neutral positions, but may restrain hip ROM in individuals with cam morphology. However, knowing that capsular ligaments also play a vital role in minimizing edge loading [59, 60], poorly functioning ligaments may be unable to prevent adverse contact loading at higher amplitudes of motion. Therefore, it would be imperative to further examine the effects of the surrounding capsule on limiting adverse stresses and microinstability [20, 32]. Finally, we examined level walking and, although there were differences in cartilage stresses among the subgroups, we did not note any substantial subchondral bone stresses. The baseline bone densities for each model were within the range of typical values for cortical and trabecular bone. There were no differences in elastic modulus between participants within a subgroup. The symptomatic and asymptomatic participants had marginally higher elastic moduli than the control group, but no differences were observed in the subchondral bone. It would be important to examine other activities that require larger hip motions (eg, squatting, stair ascent/descent) to compare if elevated subchondral bone stresses are different among subgroups and delineate pathomechanical arthritic changes [29, 52, 53]. It is hypothesized that impinging motions may cause higher stresses not only to the articulating cartilage, but also to the subchondral bone. This would further reinforce the theory that early subchondral bone adaptation may lead to secondary cartilage degeneration [42].

As mentioned, there was an overlap in femoral neck-shaft angles between the symptomatic and asymptomatic groups. The symptomatic cohort that we were selecting from did not have a high femoral neck-shaft angle and, similarly, the asymptomatic and control participants did not have low femoral neck-shaft angles for direct comparisons. The resultant consequence of these small differences has yet to be fully elucidated. The asymptomatic participants' moderate stresses were higher than the control subjects but were more evenly distributed than the symptomatic models. To our knowledge, no study has investigated hip contact stresses resulting from an asymptomatic cam morphology [36]. In one of the first finite element studies in this area, Chegini and associates [8] examined cartilage stresses using an idealized ball-and-socket model parameterized to various cam and acetabular coverage morphologies, applying instrumented prosthesis loads. They reported no changes in stress as alpha angles were increased, which may be attributed to their idealized geometry. Our results for the control subjects were slightly higher than their control parameters (contact pressure = 2.57 $\pm$ 0.89 MPa); however, we included subject-specific geometries, bone material properties, and, more importantly, joint loading, which could have yielded a higher result. Another earlier study on FAI applied subject-specific intersegmental hip forces during maximal squat [37]. Our resultant contact stresses were within a reasonable range during the lower amplitude of hip motion, but cannot directly compare with the different squatting activity. The current study considered hip contact forces as opposed to intersegmental forces from inverse dynamics, thus improving the representation of hip contact stresses. Jorge and associates [18] found much higher cartilage contact pressures at higher amplitudes of hip motion. However, their study was limited to one male subject with a severe cam deformity (age = 27 years, alpha angle = 98°) matched with one healthy female control subject (age = 50 years, alpha angle = 48°). A recent study by Hellwig and associates [15] also implemented idealized geometries and instrumented prosthesis loads during walking to compare one cam (alpha angle = 74°) with one control hip (alpha angle = 40°). Using a poroelastic, orthotropic cartilage model, they found peak contact pressures in the superior cartilage for the control hip (2.87 MPa). Peak pore pressure

was also different between control (0.42 MPa, posterior cartilage) and FAI (3.76 MPa, anterosuperior cartilage). The authors remarked that their geometries were idealized for convergence.

In this study, the symptomatic and asymptomatic participants with low femoral neck-shaft angles had the highest resultant stresses in their respective subgroups. Both symptomatic participants and the asymptomatic participant with the lower femoral neck-shaft angle indicated anterolateral and posterior stress concentrations, which coincided very closely to known areas of cartilage damage [4–6], subchondral bone stiffening [53], and decreased proteoglycan content [29, 43] as a result of cam FAI. Elevated stresses of the symptomatic group could also be attributed to preexisting chondrolabral damage, resulting in incongruent articulations and unfavorable contact mechanics. The control participant, with the lower femoral neck-shaft angle, showed more favorable contact mechanics, justifying that it could be a combination of both cam and neck angle parameters that contribute to adverse stresses. Although clinical assessment of the cam deformity is usually from multiplanar imaging, it does not provide a complete picture in regard to the likelihood for the onset of degenerative symptoms. Recent work by our group suggests that differences in peak stresses between the symptomatic and asymptomatic groups further support that a decreased femoral neck-shaft angle may be an indicator of those at risk of developing early symptoms and onset of osteoarthritis [33, 34]. Also, in recent in vivo studies by Siebenrock and associates [49, 50], intertrochanteric varus osteotomies were performed on healthy ovine hips to reduce the femoral neck-shaft angle and experimentally induce mechanical cam impingement. This resulted in localized chondrolabral degeneration, comparable to progressive damage in human hips with FAI. The coxa vara construct seated the femoral head further into the acetabulum and brought the cam morphology closer to the anterolateral and anterosuperior labrum. This may predispose to early labral damage and perhaps explain why some asymptomatic individuals do not experience early symptoms. Although the cam morphology rarely impinges at lower amplitudes of motion, the effect of a lower femoral neck-shaft angle and shortened abductor may contribute to more adverse contact loading to stabilize the pelvis during level walking [58, 61, 62]. We retrospectively examined the participants' terminal stance phase and remarked that both asymptomatic participants along with the control participant with high femoral neck-shaft angle all had higher hip extensions. Interestingly, both symptomatic individuals had small hip extensions during terminal stance, which may have been limited by capsular ligaments or perhaps indicate a protective mechanism to minimize anterior hip contact forces [25, 61]. This could be a neuromuscular adaptation mechanism to avoid pain by altering the direction and magnitude of the force vectors [30]. The unaffected, contralateral hip of the symptomatic group should be further investigated to confirm asymmetry and if compensatory load is applied onto the unaffected hip [48].

In conclusion, our study suggests that individuals with cam morphology and varus neck angle may be subjected to elevated mechanical stresses. Although asymptomatic participants had elevated stresses, a higher femoral neck-shaft angle was associated with lower stresses despite cam morphology. Thus, individuals with an asymptomatic cam morphology and low femoral neck-shaft angle may be at a greater risk of developing clinical signs and symptoms. Future studies will involve higher amplitudes of hip and pelvic motions as well as contact stresses at the underlying subchondral bone to better understand the contributions of various anatomic and functional parameters in individuals with cam morphology.

Acknowledgments We thank Kawan S. Rakhra MD, from the Department of Diagnostic Radiology, for his help with CT readings; Zlatko Lovrenovic BASc, from the Department of Mechanical Engineering, for his help with segmentation and modeling; and Jae-Jin Ryu PhD, from The Ottawa Hospital's Division of Orthopedic Surgery, for her help with patient recruitment.

References

1. Agricola R, Heijboer MP, Bierma-Zeinstra SM, Verhaar JA, Weinans H, Waarsing JH. Cam impingement causes osteoarthritis of the hip: a nationwide prospective cohort study (CHECK). *Ann Rheum Dis*. 2012;72:918–923.
2. Allen D, Beaule PE, Ramadan O, Doucette S. Prevalence of associated deformities and hip pain in patients with cam-type femoroacetabular impingement. *J Bone Joint Surg Br*. 2009;91:589–594.
3. Ateshian GA, Ellis BJ, Weiss JA. Equivalence between short-time biphasic and incompressible elastic material responses. *J Biomech Eng*. 2007;129:405–412.
4. Beaulé P, Hynes K, Parker G, Kemp K. Can the alpha angle assessment of cam impingement predict acetabular cartilage delamination? *Clin Orthop Relat Res*. 2012;470:3361–3367.
5. Beaule PE, Zaragoza E, Motamedi K, Copelan N, Dorey FJ. Three-dimensional computed tomography of the hip in the assessment of femoroacetabular impingement. *J Orthop Res*. 2005;23:1286–1292.
6. Beck M, Kalhor M, Leunig M, Ganz R. Hip morphology influences the pattern of damage to the acetabular cartilage: femoroacetabular impingement as a cause of early osteoarthritis of the hip. *J Bone Joint Surg Br*. 2005;87:1012–1018.
7. Bergmann G, Graichen F, Rohlmann A. Hip joint loading during walking and running, measured in two patients. *J Biomech*. 1993;26:969–990.
8. Chegini S, Beck M, Ferguson SJ. The effects of impingement and dysplasia on stress distributions in the hip joint during sitting and walking: a finite element analysis. *J Orthop Res*. 2009;27:195–201.
9. Delp SL, Loan JP, Hoy MG, Zajac FE, Topp EL, Rosen JM. An interactive graphics-based model of the lower extremity to study orthopaedic surgical procedures. *IEEE Trans Biomed Eng*. 1990;37:757–767.

10. Egea AJS, Valera M, Quiroga JMP, Proubasta I, Noailly J, Lacroix D. Impact of hip anatomical variations on the cartilage stress: A finite element analysis towards the biomechanical exploration of the factors that may explain primary hip arthritis in morphologically normal subjects. *Clin Biomech*. 2014;29:444–450.
11. Ganz R, Parvizi J, Beck M, Leunig M, Nötzli H, Siebenrock KA. Femoroacetabular impingement: a cause for osteoarthritis of the hip. *Clin Orthop Relat Res*. 2003;417:112–120.
12. Hack K, Di Primio G, Rakhra K, Beaule PE. Prevalence of cam-type femoroacetabular impingement morphology in asymptomatic volunteers. *J Bone Joint Surg Am*. 2010;92:2436–2444.
13. Hartofilakidis G, Bardakos NV, Babis GC, Georgiades G. An examination of the association between different morphotypes of femoroacetabular impingement in asymptomatic subjects and the development of osteoarthritis of the hip. *J Bone Joint Surg Br*. 2011;93:580–586.
14. Heller MO, Bergmann G, Kassi JP, Claes L, Haas NP, Duda GN. Determination of muscle loading at the hip joint for use in preclinical testing. *J Biomech*. 2005;38:1155–1163.
15. Hellwig FL, Tong J, Hussell JG. Hip joint degeneration due to cam impingement: a finite element analysis. *Comput Methods Biomech Biomed Eng*. 2016;19:41–48.
16. Henak CR, Ellis BJ, Harris MD, Anderson AE, Peters CL, Weiss JA. Role of the acetabular labrum in load support across the hip joint. *J Biomech*. 2011;44:2201–2206.
17. Ito K, Leunig M, Ganz R. Histopathologic features of the acetabular labrum in femoroacetabular impingement. *Clin Orthop Relat Res*. 2004;429:262–271.
18. Jorge JP, Simoes FM, Pires EB, Rego PA, Tavares DG, Lopes DS, Gaspar A. Finite element simulations of a hip joint with femoroacetabular impingement. *Comput Methods Biomech Biomed Eng*. 2014;17:1275–1284.
19. Jung KA, Restrepo C, Hellman M, AbdelSalam H, Morrison W, Parvizi J. The prevalence of cam-type femoroacetabular deformity in asymptomatic adults. *J Bone Joint Surg Br*. 2011;93:1303–1307.
20. Kalisvaart MM, Safran MR. Microinstability of the hip—it does exist etiology, diagnosis and treatment. *J Hip Preserv Surg*. 2015;2:123–135.
21. Kennedy MJ, Lamontagne M, Beaule PE. Femoroacetabular impingement alters hip and pelvic biomechanics during gait Walking biomechanics of FAI. *Gait Posture*. 2009;30:41–44.
22. Khanna V, Caragianis A, Diprimio G, Rakhra K, Beaule PE. Incidence of hip pain in a prospective cohort of asymptomatic volunteers: is the cam deformity a risk factor for hip pain? *Am J Sports Med*. 2014;42:793–797.
23. Lamontagne M, Brisson N, Kennedy MJ, Beaulé PE. Preoperative and postoperative lower-extremity joint and pelvic kinematics during maximal squatting of patients with cam femoro-acetabular impingement. *J Bone Joint Surg Am*. 2011;93:40–45.
24. Lamontagne M, Kennedy MJ, Beaule PE. The effect of cam FAI on hip and pelvic motion during maximum squat. *Clin Orthop Relat Res*. 2009;467:645–650.
25. Lewis CL, Sahrmann SA, Moran DW. Effect of hip angle on anterior hip joint force during gait. *Gait Posture*. 2010;32:603–607.
26. Lu TW, O'Connor JJ, Taylor SJ, Walker PS. Validation of a lower limb model with in vivo femoral forces telemetered from two subjects. *J Biomech*. 1998;31:63–69.
27. Macirowski T, Tepic S, Mann RW. Cartilage stresses in the human hip joint. *J Biomech Eng*. 1994;116:10–18.
28. Mantovani G, *Hip Joint Contact Load and Muscle Force in Femoroacetabular Impingement Population.* Ottawa, Canada: University of Ottawa; 2016:182.
29. McGuffin WS, Melkus G, Rakhra KS, Beaule PE. Is the contralateral hip at risk in patients with unilateral symptomatic cam femoroacetabular impingement? A quantitative T1rho MRI study. *Osteoarthritis Cartilage*. 2015;23:1337–1342.
30. Mendis MD, Wilson SJ, Hayes DA, Watts MC, Hides JA. Hip flexor muscle size, strength and recruitment pattern in patients with acetabular labral tears compared to healthy controls. *Man Ther*. 2014;19:405–410.
31. Modenese L, Phillips AM. Prediction of hip contact forces and muscle activations during walking at different speeds. *Multibody Syst Dyn*. 2012;28:157–168.
32. Myers CA, Register BC, Lertwanich P, Ejnisman L, Pennington WW, Giphart JE, LaPrade RF, Philippon MJ. Role of the acetabular labrum and the iliofemoral ligament in hip stability: an in vitro biplane fluoroscopy study. *Am J Sports Med*. 2011;39(Suppl):85S–91S.
33. Ng KCG, Lamontagne M, Adamczyk AP, Rakhra KS, Beaule PE. Patient-specific anatomical and functional parameters provide new insights into the pathomechanism of cam FAI. *Clin Orthop Relat Res*. 2015;473:1289–1296.
34. Ng KCG, Lamontagne M, Beaulé PE. Differences in anatomical parameters between the affected and unaffected hip in patients with bilateral cam-type deformities. *Clin Biomech*. 2016;33:13–19.
35. Ng KCG, Lamontagne M, Labrosse MR, Beaulé PE. Comparison of anatomical parameters of cam femoroacetabular impingement to evaluate hip joint models segmented from CT data. *Comput Methods Biomech Biomed Eng Imaging Vis.* 2016; in press. DOI 10.1080/21681163.2016.1216805.
36. Ng KCG, Lamontagne M, Labrosse MR, Beaulé PE. Hip joint stresses due to cam-type femoroacetabular impingement: a systematic review of finite element simulations. *PLoS One*. 2016;11:e0147813.
37. Ng KCG, Rouhi G, Lamontagne M, Beaulé PE. Finite element analysis examining the effects of cam FAI on hip joint mechanical loading using subject-specific geometries during standing and maximum squat. *HSS J*. 2012;8:206–212.
38. Nötzli HP, Wyss TF, Stoecklin CH, Schmid MR, Treiber K, Hodler J. The contour of the femoral head-neck junction as a predictor for the risk of anterior impingement. *J Bone Joint Surg Br*. 2002;84:556–560.
39. Pandy MG. Computer modeling and simulation of human movement. *Annu Rev Biomed Eng*. 2001;3:245-273.
40. Park S, Hung CT, Ateshian GA. Mechanical response of bovine articular cartilage under dynamic unconfined compression loading at physiological stress levels. *Osteoarthritis Cartilage*. 2004;12:65–73.
41. Prilutsky BI, Zatsiorsky VM. Optimization-based models of muscle coordination. *Exerc Sport Sci Rev*. 2002;30:32–38.
42. Radin EL, Paul IL, Tolkoff MJ. Subchondral bone changes in patients with early degenerative joint disease. *Arthritis Rheum*. 1970;13:400–405.
43. Rakhra KS, Lattanzio PJ, Cardenas-Blanco A, Cameron IG, Beaule PE. Can T1-rho MRI detect acetabular cartilage degeneration in femoroacetabular impingement? A pilot study. *J Bone Joint Surg Br*. 2012;94:1187–1192.
44. Rakhra KS, Sheikh AM, Allen D, Beaule PE. Comparison of MRI alpha angle measurement planes in femoroacetabular impingement. *Clin Orthop Relat Res*. 2009;467:660–665.
45. Ranawat A, Schulz B, Baumbach S, Meftah M, Ganz R, Leunig M. Radiographic predictors of hip pain in femoroacetabular impingement. *HSS J*. 2011;7:115–119.
46. Rubin DA. Femoroacetabular impingement: fact, fiction, or fantasy? *AJR Am J Roentgenol*. 2013;201:526–534.
47. Schileo E, Dall'ara E, Taddei F, Malandrino A, Schotkamp T, Baleani M, Viceconti M. An accurate estimation of bone density

improves the accuracy of subject-specific finite element models. *J Biomech*. 2008;41:2483–2491.
48. Shakoor N, Dua A, Thorp LE, Mikolaitis RA, Wimmer MA, Foucher KC, Fogg LF, Block JA. Asymmetric loading and bone mineral density at the asymptomatic knees of patients with unilateral hip osteoarthritis. *Arthritis Rheum*. 2011;63:3853–3858.
49. Siebenrock KA, Fiechter R, Tannast M, Mamisch TC, von Rechenberg B. Experimentally induced cam impingement in the sheep hip. *J Orthop Res*. 2013;31:580–587.
50. Siebenrock KA, Kienle KP, Steppacher SD, Tannast M, Mamisch TC, von Rechenberg B. Biochemical MRI predicts hip osteoarthritis in an experimental ovine femoroacetabular impingement model. *Clin Orthop Relat Res*. 2015;473:1318–1324.
51. Speirs AD, Beaule PE, Ferguson SJ, Frei H. Stress distribution and consolidation in cartilage constituents is influenced by cyclic loading and osteoarthritic degeneration. *J Biomech*. 2014;47: 2348–2353.
52. Speirs AD, Beaule PE, Rakhra KS, Schweitzer ME, Frei H. Bone density is higher in cam-type femoroacetabular impingement deformities compared to normal subchondral bone. *Osteoarthritis Cartilage*. 2013;21:1068–1073.
53. Speirs AD, Beaule PE, Rakhra KS, Schweitzer ME, Frei H. Increased acetabular subchondral bone density is associated with cam-type femoroacetabular impingement. *Osteoarthritis Cartilage*. 2013;21:551–558.
54. Steele KM, Seth A, Hicks JL, Schwartz MS, Delp SL. Muscle contributions to support and progression during single-limb stance in crouch gait. *J Biomech*. 2010;43:2099–2105.
55. Sutter R, Dietrich TJ, Zingg PO, Pfirrmann CWA. How useful is the alpha angle for discriminating between symptomatic patients with cam-type femoroacetabular impingement and asymptomatic volunteers? *Radiology*. 2012;264:514–521.
56. Taddei F, Schileo E, Helgason B, Cristofolini L, Viceconti M. The material mapping strategy influences the accuracy of CT-based finite element models of bones: an evaluation against experimental measurements. *Med Eng Phys*. 2007; 29:973–979.
57. Unsworth A, Dowson D, Wright V. The frictional behavior of human synovial joints—part I: natural joints. *Journal of Lubrication Technology—Transactions of ASME*. 1975;97:369–376.
58. Valente G, Taddei F, Jonkers I. Influence of weak hip abductor muscles on joint contact forces during normal walking: probabilistic modeling analysis. *J Biomech*. 2013;46:2186–2193.
59. van Arkel RJ, Amis AA, Cobb JP, Jeffers JR. The capsular ligaments provide more hip rotational restraint than the acetabular labrum and the ligamentum teres: an experimental study. *Bone Joint J*. 2015;97:484–491.
60. van Arkel RJ, Amis AA, Jeffers JR. The envelope of passive motion allowed by the capsular ligaments of the hip. *J Biomech*. 2015;48:3803–3809.
61. Wesseling M, de Groote F, Meyer C, Corten K, Simon JP, Desloovere K, Jonkers I. Gait alterations to effectively reduce hip contact forces. *J Orthop Res*. 2015;33:1094–1102.
62. Wesseling M, Meyer C, de Groote F, Corten K, Simon JP, Desloovere K, Jonkers I. Gait alterations can reduce the risk of edge loading. *J Orthop Res*. 2016;34:1069–1076.
63. Wu G, Siegler S, Allard P, Kirtley C, Leardini A, Rosenbaum D, Whittle M, D'Lima DD, Cristofolini L, Witte H, Schmid O, Stokes I. ISB recommendation on definitions of joint coordinate system of various joints for the reporting of human joint motion—part I: ankle, hip, and spine. International Society of Biomechanics. *J Biomech*. 2002;35:543–548.